Dalton Transactions

Cite this: *Dalton Trans.*, 2012, **41**, 11093

www.rsc.org/dalton

PAPER

Hydrogenolysis of β-O-4 lignin model dimers by a ruthenium-xantphos catalyst†‡

Adam Wu, Brian O. Patrick, Enoch Chung and Brian R. James*

Received 16th May 2012, Accepted 25th June 2012
DOI: 10.1039/c2dt31065a

Hydrogenolysis reactions of so-called lignin model dimers using a Ru-xantphos catalyst are presented (xantphos = 4,5-bis(diphenylphosphino)-9,9-dimethylxanthene). For example, of some nine models studied, the alcohol, 2-(2-methoxyphenoxy)-1-phenylethanol (**1**), with 5 mol% $Ru(H)_2(CO)(PPh_3)$-(xantphos) (**18**) in toluene-d_8 at 135 °C for 20 h under N_2, gives in ~95% yield the C–O cleavage hydrogenolysis products, acetophenone (**14**) and guaiacol (**17**), and a small amount (<5%) of the ketone, 2-(2-methoxyphenoxy)-1-phenylethanone (**4**), as observed by ^{1}H NMR spectroscopy. The *in situ* $Ru(H)_2(CO)(PPh_3)_3$/xantphos system gives similar findings, confirming a recent report (J. M. Nichols *et al.*, *J. Am. Chem. Soc.*, 2010, **132**, 12554). The active catalyst is formulated 'for convenience' as 'Ru(CO)(xantphos)'. The hydrogenolysis mechanism proceeds by initial dehydrogenation to give the ketone **4**, which then undergoes hydrogenolysis of the C–O bond to give **14** and **17**. Hydrogenolysis of **4** to **14** and **17** also occurs using the Ru catalyst under 1 atm H_2; in contrast, use of 3-hydroxy-2-(2-methoxyphenoxy)-1-phenyl-1-propanone (**7**), for example, where the CH_2 of **4** has been changed to $CHCH_2OH$, gives a low yield (≤15%) of hydrogenolysis products. Similarly, the diol substrate, 2-(2-methoxyphenoxy)-1-phenyl-1,3-propanediol (**9**), gives low yields of hydrogenolysis products. These low yields are due to formation of the catalytically inactive complexes Ru(CO)(xantphos)[C(O)C-(OC_6H_4OMe)═C(Ph)O] (**20**) and/or Ru(CO)(xantphos)[C(O)CH═C(Ph)O] (**21**), where the organic fragments result from dehydrogenation of CH_2OH moieties in **7** and **9**. Trace amounts of Ru(CO)-(xantphos)(OC_6H_4O), a catecholate complex, are isolated from the reaction of **18** with **1**. Improved syntheses of **18** and lignin models are also presented.

Introduction

Lignocellulosic biomass is an attractive, potential renewable source of biofuels and other useful aromatic compounds.[1,2] Due to the high lignin content in wood (15–30% by weight),[3] the pulp and paper industry generates a substantial amount of lignin as a waste product, and there have been decades of research particularly, by this industry to extend the current, limited industrial uses of lignin.[4]

Lignin is an amorphous, three-dimensional organic polymer whose natural abundance is second only to that of cellulose and, when burned (the usually fate of waste lignin), has a higher energy yield than cellulose.[1,3] The disordered structure of lignin is complex, being comprised of non-identical phenolic units interconnected by a network of C–C and C–O bonds.[1–6] Selective 'depolymerisation' of lignin, for example, into smaller phenolic derivatives, could generate a beneficial source of useful materials, and this aim motivated the studies described in this paper. The predominant linkage between two aromatic groups of lignin is described as a β-O-4 linkage – see Chart 1, which shows the so-called 'dimer' lignin models[7] used in this paper to represent this linkage, which typically comprises some 50–60% of lignin structures; the lower values are found in softwoods such as spruce, with the higher values being typical of hardwoods such as birch and eucalyptus.[6]

Studies on degradation of lignin and lignin models are incessant, and are exemplified by recent reports that include bacterial degradation,[8] heterogeneous Co(salen)-catalyzed oxidation using H_2O_2 under microwave radiation,[9] and hydrolytic cleavage in an ionic liquid in the presence of $FeCl_3$, $CuCl_2$, or $AlCl_3$.[10] Other recent studies on lignin model compounds[2,11–13] that are the same as, or closely related to, the dimers shown in Chart 1, will be discussed later in the Results and discussion section.

Department of Chemistry, University of British Columbia, Vancouver, British Columbia V6T 1Z1, Canada. E-mail: brj@chem.ubc.ca

†Dedicated to Professor David Cole-Hamilton on the occasion of his retirement and for his outstanding contribution to transition metal catalysis.

‡CCDC 883563–883566 for **13** and **19–21**. For crystallographic data in CIF or other electronic format see DOI: 10.1039/c2dt31065a

xantphos

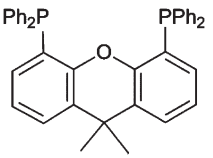

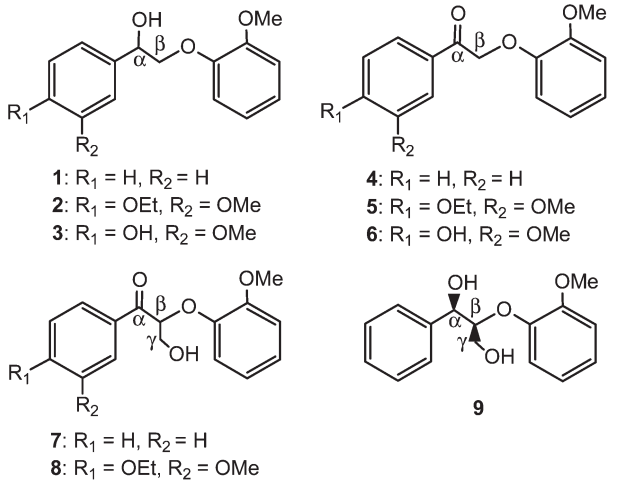

Chart 1 β-O-4 (**1–6**) and β-O-4/γ-OH (**7–9**) lignin model dimers. The α, β, and γ positions are defined with respect to an aromatic ring, and the '4' to the para position of the second aromatic ring, which in lignin structures is part of a polymer chain; 'dimer' implies the presence of two aromatic groups.

A key report in 2010 that prompted our studies was that of Bergman, Ellman and co-workers,[14] who used an *in situ* $Ru(H)_2(CO)(PPh_3)_3$/xantphos catalyst *under* N_2 for the reactions shown below, where a β-O-4 aryl dimer (eqn (1)) or polymer (eqn (2)) is cleaved into monomers in high yields; xantphos is the wide bite-angle diphosphine, 4,5-bis(diphenylphosphino)-9,9-dimethylxanthene. The process involves initial dehydrogenation of a CH(OH) moiety to C(O), followed by hydrogenolysis of the CH_2–OAr′ bond. Our paper presents further studies on the reactivity of this catalyst system (under H_2 as well as N_2) with lignin β-O-4 aryl dimer models with and without the γ-OH group functionality (**1–9** shown in Chart 1). Data include three X-ray structures of Ru-xantphos complexes with organic fragments, which aid in discussing plausible, catalytic hydrogenolysis mechanisms.

$$\mathrm{ArCH(OH)CH_2OAr'} \xrightarrow{-H_2} [\mathrm{ArC(O)CH_2OAr'}] \xrightarrow{+H_2} \mathrm{ArC(O)CH_3 + HOAr'} \quad (1)$$

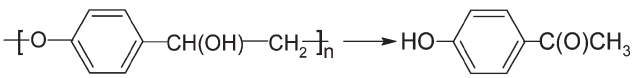

(2)

More generally, the chemistry of Ru(xantphos) species has been reported since 2001, and has included structural data on complexes with *N*-heterocyclic carbenes,[15] hydrides,[16,17] and DMSO[18] as auxiliary ligands, as well as reports on catalytic processes such as olefin metathesis,[19] alkylation of alcohols with activated methylene compounds,[20] conversions of 1,4-alkynediols into 2,5-disubstituted furans, pyrroles, and pyridazines,[21] conversion of oxime ethers into nitriles,[22] syntheses of benzazoles and other heterocycles,[23] and hydroformylation processes.[24]

Results and discussion

Synthesis of lignin models

Of the compounds shown in Chart 1, 2-(2-methoxyphenoxy)-1-phenylethanol (**1**) and the 1-phenylethanone analogue (**4**),[14] and 1-(4-ethoxy-3-methoxyphenyl)-2-(2-methoxyphenoxy)ethanone (**5**) and the 1-propanone analogue (**8**)[11] were made according to literature methods. Borohydride reduction of the carbonyl moiety in **5** (as used in formation of **1** from **4**)[14] gave the alcohol **2** in 77% yield, and **7** (3-hydroxy-2-(2-methoxyphenoxy)-1-phenyl-1-propanone) was made in 26% yield by reaction of **4** with HCHO and K_2CO_3 (as used for synthesis of **8** from **5**).[11]

Compounds **3** and **6** were synthesized using modified literature procedures as summarised in Scheme 1.[25–27] Reaction of acetovanillone with benzoyl chloride, pyridine and Br_2 in $CHCl_3$ gives 4-benzoyl-3-methoxy-bromoacetylbenzene (**10**) which with guaiacol and K_2CO_3 in acetone produces **11**. Treatment of **11** with NaOH and $NaBH_4$ in THF/H_2O yields **3** directly, whereas treatment with just NaOH yields **6**; in both cases, the NaOH converts the protecting OBz group to OH.

The new compounds (**2**, **3**, **6**, and **7**) were well characterized by ^1H and $^{13}C\{^1H\}$NMR spectroscopy, and ESI/MS; the elemental analyses were satisfactory after including in the formulations up to 0.5 mol of H_2O, which was detected in the ^1H NMR spectra.

2-(2-Methoxyphenoxy)-1-phenyl-1,3-propanediol (**9**) was synthesized (see Scheme 2) following methods used for analogous compounds.[11,12,28] Guaiacol with methylbromoacetate gives **12** (a 2-substituted acetate) that was reacted in THF with lithium diisopropylamide (LDA) and benzaldehyde to give **13**; this was initially isolated as a yellow oil that was converted into a white powder by treatment with a mixture of CH_2Cl_2 and hexanes. Crystals of **13** were grown by slow evaporation of a CH_2Cl_2 solution of the powder layered with hexanes. Some X-ray crystallographic data are given in Table 1, and Fig. 1 shows an ORTEP diagram of the structure; this reveals a racemic mixture of the 2*R*,3*R*- and 2*S*,3*S*-erythro diastereomers that result from the two chiral carbon centres. The ^1H and $^{13}C\{^1H\}$ NMR spectra of **13** show the presence of only one set of signals, consistent with such a mixture. The analogous compounds, methyl 3-(4-ethoxy-3-methoxyphenyl)-3-hydroxy-2-(2-methoxyphenoxy)propanoate[11] and ethyl 3-hydroxy-3-(3,5-dimethoxyphenyl)-2-(2-methyoxyphenoxy)propanoate[12] have also been isolated mainly as an assigned erythro diastereomer; the stereochemical assignments for these types of compounds are well established.[29] Borohydride reduction of **13** produced **9** that was isolated as a viscous yellow oil, whose ^1H and $^{13}C\{^1H\}$ NMR data reveal a major to minor diastereomer ratio of 9 : 1; data are only given in the Experimental section for the major isomer, presumably a racemic mixture of the 1*R*,2*S*- and 1*S*,2*R*-erythro diastereomers. The same assignment has been proposed for the products from borohydride reduction of the 'analogous compounds' mentioned above.[11,12] Compound **9** has been synthesized by a different route that gave a 1 : 1 mixture of diastereomers.[30] It seems likely that the crystallization process to convert **13** from an oil to a white solid results in a separation process that gives solely the 2*R*,3*R*/2*S*,3*S* racemic mixture.

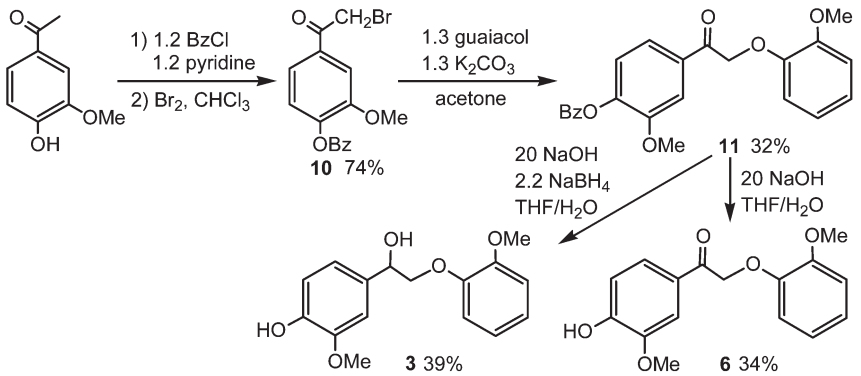

Scheme 1 Synthetic routes to, and yields of, **3** and **6**.

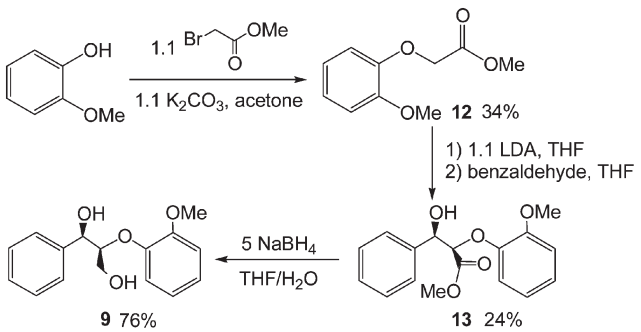

Scheme 2 Synthetic routes to, and yields of, **9**.

Catalysed hydrogenolysis of 1–3

Reaction of **1** (0.20 M) with 5 mol% *in situ* [$Ru(H)_2(CO)(PPh_3)_3$/xantphos] or the isolated $Ru(H)_2(CO)(PPh_3)$(xantphos) (**18**)[16] in toluene-d_8 at 135 °C for 20 h *under N_2 or Ar* gives quantitative conversion and high yields of the hydrogenolysis products, acetophenone (**14**) and guaiacol (**17**), and ≤5% of the ketone dimer **4** (Scheme 3; Table 2, entries I and V); this substrate was studied previously using the *in situ* system,[14] and the two sets of data agree well. In essence, **1** has been dehydrogenated to give **4**, which then undergoes hydrogenolysis of the C–O bond to form **14** and **17** (see next section). No reaction was seen in the absence of a Ru catalyst (xantphos itself was also inactive), while $Ru(H)_2(CO)(PPh_3)_3$ was a much less active catalyst (entry IX). With either the *in situ* system or **18** as catalyst, **2** similarly gives quantitative conversion and high yields of **15** and **17**, with some formation of ketone **5** (Table 2, entries II and VI). Substrate **3**, the phenol substituted model, is also quantitatively converted, but with lower yields of acetovanillone (**16**) and **17** and a higher yield of intermediate **6** (17–21%) (Table 2, entries III and VII), implying a lower rate for hydrogenolysis of this ketone. These differences are difficult to rationalize, but are more marked for the *in situ* catalyst systems, where the presence of two uncoordinated PPh_3 per Ru could play a role. Under 1 atm H_2, the same 2-stage process is still seen for substrate **1** with the xantphos catalyst systems (Table 2, entries IV and VIII), but now the initially formed acetophenone undergoes hydrogenation to 1-phenylethanol and the intermediate ketone **4** is not seen; of interest, no reactions are observed when $Ru(H)_2(CO)(PPh_3)_3$ was tested for catalytic activity under H_2.

Catalysed H_2-hydrogenolysis of 4–6

The ketones **4–6**, under the same conditions used for studying substrates **1–3**, but under H_2 instead of N_2 (see above), are efficiently catalytically converted to **14–16**, respectively, and the same co-product, guaiacol (**17**) (*cf.* Scheme 3; Table 3, entries I–III). The findings confirm the 2-stage dehydrogenation–hydrogenolysis catalytic process for the alcohol substrates **1–3**; this implies formation of a 'Ru-xantphos dihydride' in the 1st-stage, this species then utilizing the 'dihydride' for the hydrogenolysis of the intermediate ketone. Under N_2, hydrogenolysis of **4** (Table 3, entry IV) gives low conversion and yields, confirming that H_2 is required for the catalytic process. Of note is that no alcohols are formed from the observed ketone products **14–16**, although data from Table 2 (entries IV and VIII) show clearly that this hydrogenation reaction is catalysed by the Ru-xantphos species; these findings imply that the hydrogenolysis of ketones **4–6** occurs more readily, perhaps because these coordinate more strongly than **14–16** to Ru. Control experiments (*e.g.* absence of Ru) gave zero conversions. Reaction of **4** with $Ru(H)_2(CO)(PPh_3)_3$ under N_2 (entry V) shows low activity, while under H_2 (Table 3, entry VI) higher conversion was seen but this results from significant hydrogenation to the corresponding alcohol **1**. Thus, effective hydrogenolysis of **4** requires the Ru-xantphos catalyst and hydrogen, provided by either H_2 gas or an alcohol source exemplified by substrates **1–3**. The hydrogenolysis catalysis within Scheme 3 was less effective in the presence of air or O_2, and was not studied in any detail.

Mechanistic insight into catalysed reactions of 1 and 4

The relevant chemistry catalysed by complex **18** (Scheme 3) shows that the alcohol **1** is dehydrogenated to give the ketone **4**, which subsequently undergoes C–O cleavage by hydrogenolysis to give acetophenone (**14**) and guaiacol (**17**); and this all takes place *under N_2 or Ar*. One assumes that the initial dehydrogenation of **1** cannot involve the dihydride **18**, which likely acts as a precursor to the actual catalytic species. Indeed, heating a toluene-d_8 solution of **18** at the catalytic conditions under Ar results in a colour change from yellow to reddish orange. ^1H NMR data at room temperature (r.t.) of this solution (using hexamethylbenzene as a standard) show loss of the hydride signals of **18** (δ_H −6.68 and −8.73), while the coordinated xantphos-Me

Table 1 X-ray crystallographic data for **13** and **19–21**

	13	**19**·CH_2Cl_2	**20**	**21**
Empirical formula	$C_{17}H_{18}O_5$	$C_{47}H_{38}O_4RuP_2Cl_2$	$C_{56}H_{44}O_6P_2Ru$	$C_{49}H_{38}O_4P_2Ru$
Fw	302.31	900.68	975.92	853.80
Crystal dimensions (mm)	0.10 × 0.19 × 0.43	0.08 × 0.10 × 0.22	0.08 × 0.17 × 0.28	0.04 × 0.20 × 0.24
Crystal system	Monoclinic	Monoclinic	Monoclinic	Monoclinic
Space group	$P2_1$(#4)	$P2_1/m$(#11)	$P2_1/c$(#14)	$P2_1/c$(#14)
a (Å)	5.4510(3)	9.689(2)	11.3989(6)	17.647(4)
b (Å)	15.0943(9)	14.871(3)	35.688(2)	38.343(8)
c (Å)	18.123(1)	14.223(3)	12.4658(7)	11.412(2)
α (°)	90	90	90	90
β (°)	93.661(2)	99.352(3)	116.645(1)	91.182(4)
γ (°)	90	90	90	90
Volume (Å^3)	1488.1(2)	2213.1(6)	1114.6(2)	7720(3)
Z	4	2	4	8
Density (g cm^{-3}, calcd)	1.349	1.479	1.430	1.469
μ (cm^{-1})	8.23	6.44	4.70	5.36
Reflections collected	27 755	79 814	60 850	180 811
Unique reflections	5231	6130	10 803	15 985
R_{int}	0.031	0.043	0.059	0.108
R_1, wR_2	0.035, 0.090	0.031, 0.081	0.066, 0.109	0.102, 0.231
Goodness of fit	1.03	1.04	1.13	1.26

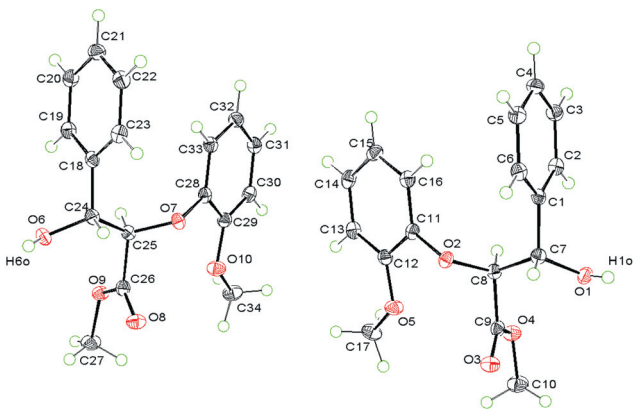

Fig. 1 ORTEP diagram of **13** as erythro racemates (2*R*,3*R* at left and 2*S*,3*S* at right). Selected bond lengths (Å) and angles (°) for the 2*S*,3*S*-diastereomer: C(7)–O(1) 1.4303(19), C(7)–C(8) 1.529(2), C(8)–O(2) 1.4288(18), C(11)–O(2) 1.3906(18), C(8)–C(9) 1.525(2), C(9)–O(3) 1.2011(19), C(9)–O(4) 1.3377(19), C(10)–O(4) 1.4455(18); O(1)–C(7)–C(8) 105.55(11), O(2)–C(8)–C(7) 106.83(11), C(11)–O(2)–C(8) 114.26 (11), O(2)–C(11)–C(12) 119.27(13), O(2)–C(8)–C(9) 110.87(12), O(3)–C(9)–O(4) 125.11(14), C(9)–O(4)–C(10) 115.60(12).

singlets of **18** (δ_H 1.38 and 1.51) are replaced by a complex, broad set of signals at δ_H 0.80–1.51. The two multiplet $^{31}P\{^1H\}$ signals of **18** (δ_P ~31 and ~46) are replaced by weak broad signals at δ_P ~52 and about −22,[31,32] with a sharp singlet being seen for free PPh_3 (δ_P −4.7); the one mole of PPh_3 per mol Ru was quantified by use of an external, capillary standard of O=PPh_3 (δ_P 27.5 in CD_3CN). The NMR spectra at −50 °C revealed trace broad hydride signals in the δ_H −8 to −10 region, while further weak $^{31}P\{^1H\}$ signals were seen in the δ_P 60 to −20 region. Treatment of the reddish orange solution with 1 atm H_2 at r.t. regenerated a yellow colour, and the NMR data now showed ~10% of **18**, other broad hydride signals (δ_H −8.0 and −9.5), and multiple signals in the 0.5–1.5 region for the Me groups; $^{31}P\{^1H\}$ signals were only seen for free PPh_3. Heating this solution at 135 °C for 30 min resulted in little change in the subsequently measured r.t. NMR spectra. Similar ill-defined NMR spectra (hydride signals in the δ_H −6.5 to −10.2 region, and usually just the δ_P signal for PPh_3) were observed for solution samples taken during the catalytic reactions of **18** with **1** and **4** under N_2 or H_2, the sample solutions now being green. A reported H/D exchange also provides evidence for loss of H_2 from **18**, even at 50 °C.[16]

The inorganic and organometallic chemistry of these systems is clearly extremely complicated, but it seems that under N_2, both H_2 and PPh_3 can dissociate from **18**, leaving a catalyst species that would be 'Ru(CO)(xantphos)', formally d^8–Ru^0. There seems to be reversible loss of H_2 from **18**, although PPh_3 is permanently dissociated and so other uncharacterized hydride species must be involved. The broadened NMR signals of the Ru species could be consistent with reversible processes (with H_2 and/or substrates and products), and fluxionality of the xantphos (2- and/or 3-coordinate with *cis* or *trans* P-atoms – see next section), as well as possible involvement of orthometallated species[31] and/or solvated species. The presence of a tetrahedral, paramagnetic d^8-species could also complicate the NMR spectra, but no such Ru species is known. The involvement of radical processes was ruled out in that addition of BHT (butylated hydroxytoluene = 2,6-ditertiarybutyl-4-methylphenol), a radical inhibitor, to the systems of Tables 2 and 3 (entry I) had no effect, in agreement with the communication by Nichols *et al.*[14] The isolated Ru-substrate complexes **19–21** (see below) all contain the Ru(CO)(xantphos) core, and there seems little doubt this entity is present in some form throughout the catalysis.

In the proposed, speculative mechanism (Scheme 4), **1** oxidatively adds to 'Ru(CO)(xantphos)', formed from **18**, to give **A**, a hydrido-alkoxide; extraction of the hydrogen on the α-carbon then forms a dihydrido-ketone complex (**B**), which can dissociate H_2 and the ketone **4** (observed as an intermediate product) to regenerate 'Ru(CO)(xantphos)'. The dissociation processes must be reversible to allow for the observed hydrogenolysis of **4** under H_2, which is effected through **B** by C–O bond

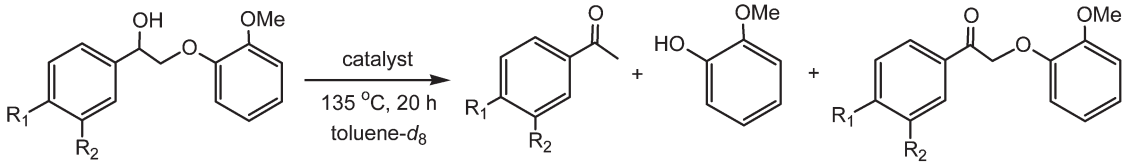

Scheme 3 Catalysed hydrogenolysis of **1–3**.

Table 2 Catalysed hydrogenolysis of **1–3** (see Scheme 3)

Entry	Substrate[a]	Catalyst	Gas[b]	Conversion[c]	**14/15/16**[c]	**17**	**4/5/6**[c]
I	**1**	[d]	N_2 or Ar	100	97–98	93	0–3
II	**2**	[d]	N_2	100	91	90	7
III	**3**	[d]	N_2	100	54	68	21
IV	**1**	[d]	H_2	91	44[g]	87	0
V	**1**	[e]	N_2 or Ar	100	95–99	93–97	0–5
VI	**2**	[e]	N_2	100	77	79	12
VII	**3**	[e]	N_2	100	63	76	17
VIII	**1**	[e]	H_2	100	27[h]	95	0
IX	**1**	[f]	N_2	29	7	10	19

[a] 0.20 M. [b] 1 atm. [c] Average % conversion/yield (by ^{1}H NMR integration) of duplicate experiments. [d] 5 mol% [$Ru(H)_2(CO)(PPh_3)_3$/xantphos]. [e] 5 mol% $Ru(H)_2(CO)(PPh_3)$(xantphos) (**18**). [f] 5 mol% $Ru(H)_2(CO)(PPh_3)_3$. [g] Yield of $PhCH(OH)CH_3$ = 39%. [h] Yield of $PhCH(OH)CH_3$ = 61%.

Table 3 Catalysed hydrogenolysis of **4–6** (*cf.* Scheme 3)

Entry	Substrate[a]	Catalyst	Gas[b]	Conversion[c]	**14/15/16**[c]	**17**[c]
I	**4**	[d,e]	H_2	100	77–85	88–89
II	**5**	[d,e]	H_2	90–100	79–89	88–99
III	**6**	[d,e]	H_2	77–91	68–83	75–90
IV	**4**	[d,e]	N_2	17–23	8–13	15
V	**4**	[f]	N_2	13	8	13
VI	**4**	[f]	H_2	63	11[g]	16

[a] 0.20 M. [b] 1 atm. [c] Average % conversion/yield (by ^{1}H NMR integration) of duplicate experiments. [d] 5 mol% [$Ru(H)_2(CO)(PPh_3)_3$/xantphos]. [e] 5 mol% $Ru(H)_2(CO)(PPh_3)$(xantphos) (**18**). [f] 5 mol% $Ru(H)_2(CO)(PPh_3)_3$. [g] Yield of **1** = 47%.

cleavage; loss of the guaiacol (**17**) from **B** requires β-carbon migration to give $RuH(CH_2C(O)Ph)(CO)$(xantphos) (**C**), which then undergoes reductive elimination of acetophenone (**14**) again with regeneration of 'Ru(CO)(xantphos)'. The proposed steps in Scheme 4 for the dehydrogenation of **1** follow those postulated in previous studies on long recognised, Ru-catalysed dehydrogenation of alcohols to ketones[16,33,34] and, of note, more recently documented, homogeneously catalysed C–O hydrogenolysis processes are dominated by ones involving Ru-phosphine species.[14,35] The proposed β-carbon migration follows that previously suggested in the *in situ* $Ru(H)_2(CO)(PPh_3)_3$/xantphos system (eqn (3)), where the product was described as the Ru-enolate tautomer that had been formed *via* a postulated Ru-monohydride catalyst.[14] This study also suggested for the subsequent hydrogenolysis step release of the ketone $ArC(O)CH_3$ prior to subsequent loss of Ar′OH,[14] whereas Scheme 4 shows loss of first the guaiacol and then acetophenone; evidence for this preference is presented later, where the structure of complex **21** is addressed. Ruthenium-catalysed hydrogenolysis of C–C bonds has more typically involved heterogeneous systems.[36]

$$Ru–O{=}C(Ar)CH_2–OAr' \rightarrow Ar'O–Ru–CH_2–C(O)–Ar \quad (3)$$

Ru^{II}–xantphos–catecholate complex (19)

After reactions involving **1** (Scheme 3, Table 2), small amounts of a yellow precipitate were observed. The same solid was formed in 17% yield from a scaled-up reaction under the same conditions using **1** and 20 mol% **18**, and then in 66% yield from a synthetic scale reaction of **18** with catechol. Crystals of **19** were grown by layering hexanes onto a CH_2Cl_2 solution of the complex. The X-ray structure (Table 1, Fig. 2) shows that **19** is $Ru(CO)$(xantphos)(OC_6H_4O) with distorted octahedral coordination involving a bidentate catecholate, a pincer-type (P–O–P)-coordinated xantphos with *cis* P-atoms, and a CO ligand that is *trans* to the oxygen. The P–Ru–P bite angle is 102.74°, similar

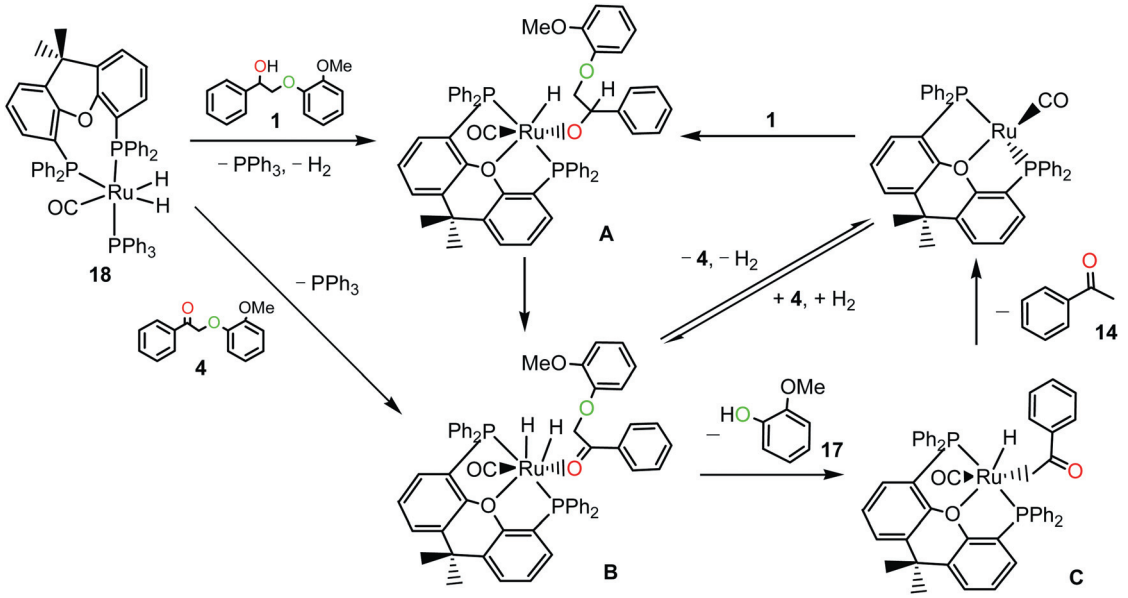

Scheme 4 Proposed mechanism for hydrogenolysis of **1** and **4** by catalyst **18**.

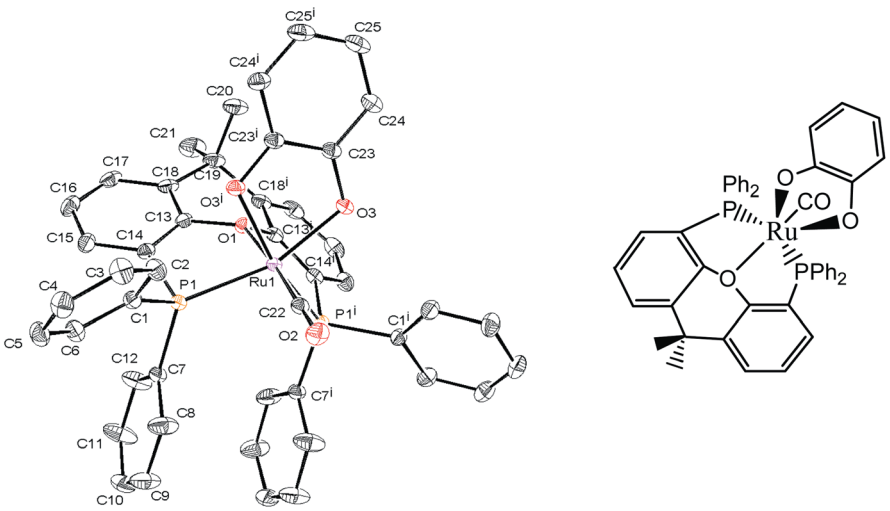

Fig. 2 ORTEP and structural diagram of Ru(CO)(xantphos)(OC_6H_4O) (**19**). Selected bond lengths (Å) and angles (°): O(1)–Ru(1) 2.1649(17), O(3)–Ru(1) 2.0723(12), P(1)–Ru(1) 2.3013(5), C(22)–Ru(1) 1.813(2); C(22)–Ru(1)–O(3) 100.33(6), O(3)–Ru(1)–O(3^i) 81.62(7), C(22)–Ru(1)–O(1) 175.24(8), O(3)–Ru(1)–O(1) 83.24(5), C(22)–Ru(1)–P(1) 95.95(5), O(3)–Ru(1)–P(1) 160.85(4), O(3^i)–Ru(1)–P(1) 85.61(4), O(1)–Ru(1)–P(1) 81.12(3), P(1)–Ru(1)–P(1^i) 102.74(3). H-atoms and a co-crystallized CH_2Cl_2 solvent molecule are not shown.

to the value of 105.48° found in *cis*-$RuCl_2$(DMSO)(xantphos), which is the only other reported Ru complex with the same tridentate mode of xantphos coordination;[18] in this complex and in **19**, the Ru–O bond length is 2.16 Å. The more common bonding mode of tridentate xantphos is with the P-atoms mutually *trans*;[17,19] complexes **20** and **21** are further examples (see later). Also reported are Ru complexes containing bidentate, P–P bound xantphos with *cis*-P atoms,[15,16] as in $Ru(H)_2(CO)(PPh_3)$(xantphos) (**18** in Schemes 4, 7 and 8).[16] The ESI/MS spectrum and elemental analysis support the formulation of **19**, whereas the NMR spectra in CD_2Cl_2 (four, equal intensity ^{1}H singlets for the Me groups, and two 1 : 1 $^{31}P\{^1H\}$ singlets at δ 49.9 and 55.1) imply the presence of two isomers in solution; these are most likely species with *cis*- and *trans*-P atoms of tridentate xantphos. The closest reported analogue of **19** is *cis*, *trans*-$Ru(CO)_2(P^iPr_3)_2(OC_6H_4O)$ which has equivalent *trans* P-atoms showing a δ_P singlet resonance at 43.4 (in C_6D_6),[37] similar to the values for **19**.

Complex **19** was also isolated in ~8% yield from the reaction of **18** with excess guaiacol (**17**) at the catalytic conditions, suggesting that the catecholate ligand derives from hydrolysis of the guaiacol **17**; thus the production of small amounts of **19** in the catalytic reactions of **1**, where **17** is formed (Scheme 3), is readily accounted for. Complex **19** is inactive as a hydrogenolysis catalyst, and at the usual catalysis conditions under N_2/Ar (Scheme 3, Table 2) simply gives ~15% conversion of **1** to the

Table 4 Catalysed reactions of **7** and **8**

Entry	Substrate[a]	Catalyst	Gas[b]	Conversion[c]	**17**[c]	**4**/**5**[c]
I	**7**	[d]	H_2 or Ar	71–81	11–15	17–23
II	**8**	[d]	H_2 or Ar	68–70	7–8	5–11
III	**7**	none	H_2 or Ar	9–12	0	3–7
IV	**7**	[e]	H_2 or Ar	24–32	0	9–13
V	**7**	[f]	H_2 or Ar	51–59	3–5	16–24

[a] 0.20 M. [b] 1 atm. [c] Average % conversion/yield (by ^{1}H NMR integration) of duplicate experiments. [d] 5 mol% **18**. [e] 5 mol% xantphos. [f] 5 mol% $Ru(H)_2(CO)(PPh_3)_3$.

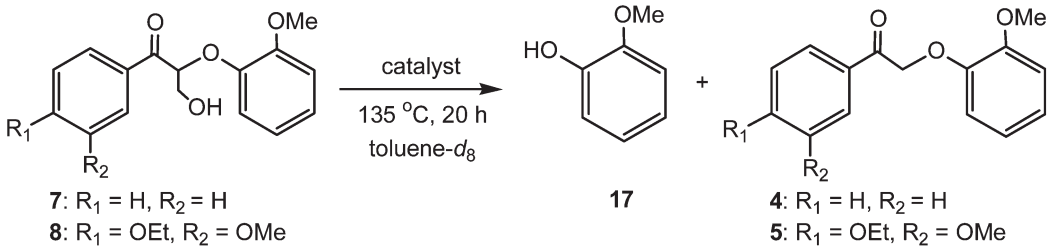

Scheme 5 Catalysed reactions of **7** and **8**.

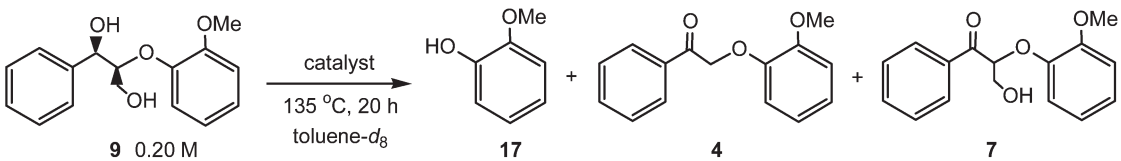

Scheme 6 Catalysed reactions of **9**.

dehydrogenated ketone product **4**. Formation of **19** thus poisons any effective catalysis; further examples of catalyst poisoning by formation of complexes **20** and **21** are discussed below.

Catalysed reactions of 7–9

Data for reactions of **7** and **8** under conditions used for substrates **1–6** are summarized in Table 4, which refers to Scheme 5. First, the data are similar whether an H_2 or Ar atmosphere was used. With the use of **18** as the catalyst, the yields of the hydrogenolysis product, guaiacol (**17**), are now only ≤15%, with similar amounts of ketones **4** or **5** being detected (Table 4, entries I and II). These ketones must be formed by loss of formaldehyde from the respective substrates **7** and **8**, the reverse process of the base-promoted synthesis of **7**/**8** by treatment of **4**/**5** with CH_2O (see Experimental section).[11] We have described above that both **4** and **5** under these catalytic conditions can undergo efficient hydrogenolysis to **17** and acetophenones (**14**/**15**) (Table 3), but such chemistry is not involved in Scheme 5. H_2 gas is not needed to form **17**, which materializes from a catalytically inactive Ru complex (see next section). In control experiments with **7** (no **18**, or in the presence of just xantphos) (Table 4, entries III and IV)), there is no production of **17**, but decomposition occurs to give up to ~10% of **4**. Trace amounts (≤5%) of **17** are formed when $Ru(H)_2(CO)(PPh_3)_3$ was used as a test catalyst for **7** under H_2 or Ar, but up to 24% decomposition to **4** is seen (entry V).

Table 5 Catalysed reactions of **9**

Entry	Catalyst	Gas[a]	Conversion[b]	**17**[b]	**4**[b]	**7**[b]
I	[c]	H_2 or Ar	73–82	11–15	3–7	7–11
II	[d]	H_2 or Ar	57–73	2–6	3–4	2–5

[a] 1 atm. [b] Average % conversion/yield (by ^{1}H NMR integration) of duplicate experiments. [c] 5 mol% **18**. [d] 5 mol% $Ru(H)_2(CO)(PPh_3)_3$.

Of note, the conversions of **7** and **8** under the various conditions range from ~10% up to 81% (Table 4), but the organic co-products along with **4**/**5** and **17** remain to be identified. The main conclusion is that the presence of a γ-OH functionality in **7** and **8** inhibits the 'simple' catalytic hydrogenolysis reactions of Scheme 3, certainly in part because of formation of the catalytically inactive complexes **20** and **21** (see below).

The same conclusion is reached when catalyst tests with substrate **9** were studied. At the usual catalytic conditions with **18** under Ar or H_2, **9** undergoes high conversion but with low yields of **17**, **4**, and **7** (Scheme 6, Table 5). The findings are similar to those seen for substrates **7** and **8** (Table 4), but are in marked contrast with data for substrates **1–3** (Table 2); the data show again that incorporation of the γ-OH group inhibits the hydrogenolysis process. Reaction of **9** with 5 mol% $Ru(H)_2(CO)(PPh_3)_3$ similarly gives trace amounts of **17**, **4**, and **7** (≤6% of

each, Table 5). Some interesting findings on the fate of the ruthenium are informative about the relative reactivities of the substrates and plausible mechanisms (see below).

Preliminary NMR experiments suggest that catalyst **18**, under the reaction conditions used for **7**–**9** (Table 4, Schemes 5 and 6) does not significantly degrade lignins.[38] The lignins contain many linkages with a γ-OH functionality;[1,5] whether this results in the formation of catalytically inactive Ru-complexes (see next section) derived from such lignin components is a key question that is currently under investigation.

Ru^{II}-xantphos catalyst/substrate complexes

Reaction of **7** (0.20 M) with **18** under the usual catalytic conditions under Ar (Scheme 5, Table 4) gives ≤15% yield of hydrogenolysis product **17** with no co-formation of acetophenone, the co-hydrogenolysis product. An explanation of this was gleaned from a scaled-up reaction of **18** with **7** under the same conditions, from which a white precipitate (complex **20**) was isolated in 34% yield. Work-up involving silica gel chromatography of the filtrate from this reaction allowed for isolation of a second white product (complex **21**) in 31% yield (Scheme 7). Layering CH_2Cl_2 and C_6H_6 solutions of **20** and **21**, respectively, with hexanes allowed for isolation of X-ray quality crystals. Monitoring an *in situ* reaction of **18** with **7** in CD_2Cl_2 by $^{31}P\{^1H\}$ NMR spectroscopy showed two singlets at δ_P 32.1 and 35.0, which correspond, respectively, to data on the isolated complexes **20** and **21**; these singlets were detected at δ_P 33.6 and 35.4 in toluene-d_8 in samples taken during the catalytic conditions.

Crystal data (Table 1) and the ORTEP diagrams for **20** and **21** (Fig. 3 and 4, respectively) show that complexes are derived from reactions of 'Ru(CO)(xantphos)' with fragments of substrate **7**. Both complexes have pseudo-octahedral structures that contain tridentate xantphos with *trans* P-atoms, with a P–Ru–P angle of ~160°. The P–P bite angle for xantphos itself is 111.7°,[39] but is clearly sufficiently flexible to bind as a tridentate ligand with the P-atoms either mutually *trans* or *cis* (see above discussion on complex **19**). The Ru–O lengths in **20** and **21** are 2.30 and 2.33 Å, respectively, surprisingly some 0.15 Å longer than in the two tridentate xantphos species with *cis* P-atoms, **19** and *cis*-$RuCl_2$(DMSO)(xantphos).[18] The other reported tridentate structures with *trans* P-atoms have Ru–O lengths in the 2.25–2.30 Å range.[17,19] The xantphos ligand seems to defy its early description of having a rigid backbone.[19,39]

The structure of **20** implies that **7** has been doubly dehydrogenated ($-2H_2$) and then coordinated *via* the γ-carbon and the enolate form of the original ketone oxygen; a plausible mechanism is considered later in Scheme 9. The structure of **21** can be described as the hydrogenolysis product of **20** with loss of guaiacol. Of interest, heating a toluene solution of **20** (NMR scale) at 135 °C for 20 h under H_2 gives low conversion (12%) to **21**, but in the reaction of **18** with **7** under Ar, **20** and **21** are formed simultaneously as evidenced by $^{31}P\{^1H\}$ NMR spectroscopy, meaning that the guaiacol is not formed *via* the hydrogenolysis of **20**. Both **20** and **21** are essentially inactive catalysts for any reactions of **7** or **1**; for example, **1** on reaction with **20** under the standard Ar/20 h conditions is just dehydrogenated to give **4** in 2% yield (*cf.* Scheme 3); the corresponding reaction using **21** under the same conditions shows ~14% conversion to give **4** (~4% yield), and hydrogenolysis products **14** (~3%) and **17** (~5%). Again, the active catalyst **18** can be 'poisoned' by conversion to **20** and **21**.

Reaction of the alcohol substrate **9** (0.20 M) with 5 mol% **18** in toluene-d_8 at 135 °C for 20 h under H_2 or Ar also gives (as does substrate **7**) ≤15% yield of guaiacol, as estimated by ^1H NMR, and the corresponding $^{31}P\{^1H\}$ NMR solution data showed formation of only **21** in ~80% yield. A scaled-up reaction under the same conditions allowed for isolation of **21** using silica gel chromatography in 23% yield (Scheme 8).

Mechanistic insight into formation of complexes 20 and 21

The catalytically inactive complexes **20** and **21** were isolated from the reaction of catalyst **18** with the ketone **7** under Ar, which gave low yields (≤15%) of the hydrogenolysis product guaiacol (**17**). Scheme 9 shows a speculative mechanism, again based on the existence of the speculative 'Ru(CO)(xantphos)' species. Similar to Scheme 4, a hydrido-alkoxide species (**D**) is formed *via* oxidative addition of the primary alcohol moiety, and subsequent hydrogen abstraction and loss of H_2 (likely *via* Ru-dihydride species) would generate the five-coordinate, Ru^0-aldehyde complex **E**. Oxidative addition of the aldehyde, which is documented for Ru^0-carbonyl-phosphine complexes,[40] would give the Ru^{II}-hydrido-acyl species **F**; loss of H_2 would result in formation of **20**, the required proton being derived from the enolate form of the ketone moiety of **F**. Alternatively, instead of H_2 loss from **F**, the '2H' is used to effect hydrogenolysis within **F** to give **17**. The simultaneous detection of **20** and **21** is consistent with their formation from a common intermediate. That only **21** is formed from substrate **9** implies loss of a further H_2 from a species analogous to **F**, but with the –C(O)Ph moiety replaced by –CH(OH)Ph, *i.e. via* a dehydrogenation process.

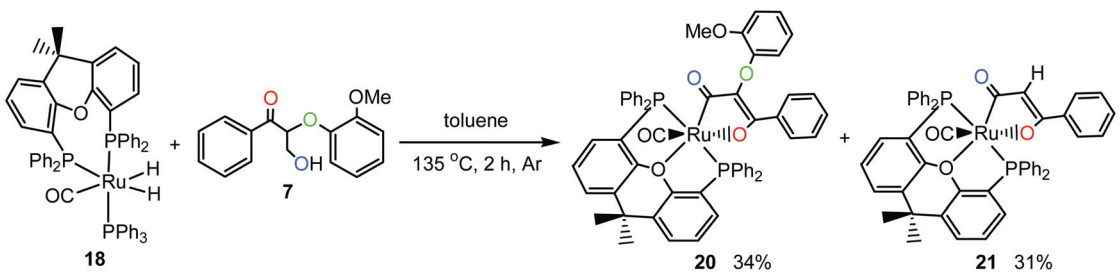

Scheme 7 Reaction of **18** with **7** to form **20** and **21**.

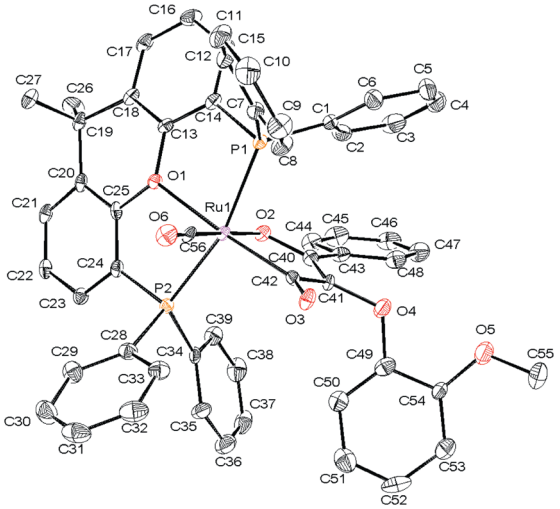

Fig. 3 ORTEP diagram of Ru(CO)(xantphos)[C(O)C(OC_6H_4OMe)═C(Ph)O] (**20**) with selected bond lengths (Å) and angles (°): C(56)–Ru(1) 1.854(3), O(1)–Ru(1) 2.2999(19), O(2)–Ru(1) 2.0871(19), P(1)–Ru(1) 2.3156(8), P(2)–Ru(1) 2.3076(8), C(42)–Ru(1) 2.003(3), C(40)–O(2) 1.314(3), C(40)–C(41) 1.371(4), C(41)–C(42) 1.471(4), C(42)–O(3) 1.229(3); C(56)–Ru(1)–C(42) 94.43(12), C(56)–Ru(1)–O(2) 177.23(10), C(42)–Ru(1)–O(2) 82.85(10), C(56)–Ru(1)–O(1) 96.79(10), C(42)–Ru(1)–O(1) 168.73(9), O(2)–Ru(1)–O(1) 85.93(7), C(56)–Ru(1)–P(2) 91.16(9), C(42)–Ru(1)–P(2) 99.57(8), O(2)–Ru(1)–P(2) 89.79(6), O(1)–Ru(1)–P(2) 81.36(5), C(56)–Ru(1)–P(1) 92.00(9), C(42)–Ru(1)–P(1) 97.89(8), O(2)–Ru(1)–P(1) 87.89(6),O(1)–Ru(1)–P(1) 80.64(5), P(2)–Ru(1)–P(1) 161.96(3). H-atoms are not shown.

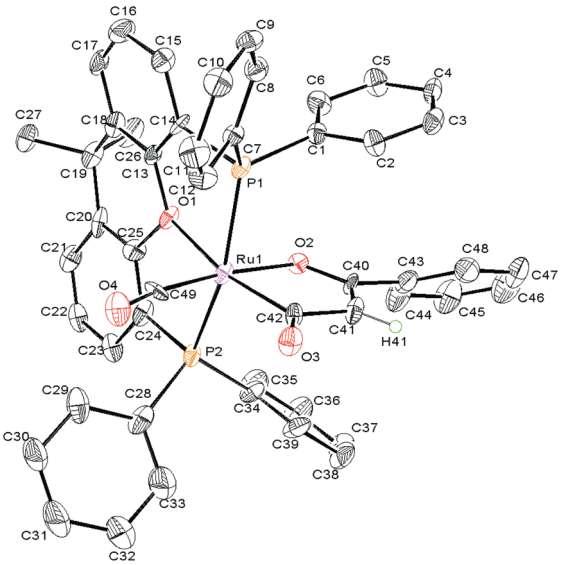

Fig. 4 ORTEP diagram of Ru(CO)(xantphos)[C(O)CH═C(Ph)O] (**21**) with selected bond lengths (Å) and angles (°): C(49)–Ru(1) 1.867(11), O(1)–Ru(1) 2.325(7), O(2)–Ru(1) 2.084(7), P(1)–Ru(1) 2.308(3), P(2)–Ru(1) 2.299(3), P(3)–Ru(2) 2.308(3), C(40)–O(2) 1.288(13), C(40)–C(41) 1.386(17), C(41)–C(42) 1.447(16), C(42)–O(3) 1.224(13); C(49)–Ru(1)–C(42) 92.6(5), C(49)–Ru(1)–O(2) 174.1(4), C(42)–Ru(1)–O(2) 82.7(4), C(49)–Ru(1)–P(2) 91.6(3), C(42)–Ru(1)–P(2) 103.0(3), O(2)–Ru(1)–P(2) 85.9(2), C(49)–Ru(1)–P(1) 94.8(3), C(42)–Ru(1)–P(1) 95.7(3), O(2)–Ru(1)–P(1) 89.3(2), P(2)–Ru(1)–P(1) 159.94(11), C(49)–Ru(1)–O(1) 101.3(4), C(42)–Ru(1)–O(1) 165.5(4), O(2)–Ru(1)–O(1) 83.6(3), P(2)–Ru(1)–O(1) 80.8(2), P(1)–Ru(1)–O(1) 79.29(19). One of two crystallographically independent molecules; H-atoms are not shown.

Related systems in catalytic degradation of lignin model compounds

Of note, vanadium-based complexes have been reported to degrade closely related, β-O-4/γ-OH lignin model dimers involving catalysed aerobic oxidation at 80–100 °C.[2,11–13] Vanadium-oxo catalysts containing, as does the Ru-xantphos system, a large bite-angle, tridentate Schiff base ligand effect in high conversion C–O cleavage within a model similar to **9** but having other OMe and OEt substituents;[11] like the Ru system (Scheme 6), the same substrate C–O bond was cleaved to give guaiacol, a 2-propene-1-one derivative, and the alkoxy-substituted **7**. A V^{IV}complex was isolated and one-electron (radical) processes involving V^{V}/V^{IV} species were favoured mechanistically,[11] in contrast to the 2e processes favoured for the Ru systems (see Schemes 4 and 9). Replacement of the Schiff base by 8-quinolinate with a closely related lignin model led to completely different selectivity involving C(phenyl)–C(alkyl) bond cleavage.[2] Related vanadium-oxo-dipicolinate systems have also been used to oxidize models such as 1-phenyl-2-phenoxy-ethanol and 1,2-diphenyl-2-methoxy-ethanol, where both C–H and C–C bond cleavage were seen, the product formation being solvent-dependent; V^{IV} species were again identified in stoichiometric reactions, and radical mechanisms were again discussed.[12,13] Data on air/O_2-oxidation of substituted ethanol models and an alkoxy-substituted **9** model catalysed by a CuCl/TEMPO system (TEMPO = tetramethylpiperidine-*N*-oxide)[12] have revealed very different product selectivities to those seen in the vanadium systems, and the Cu system required O_2 (*vs.* air) and high catalyst loading for effective rates; the findings were optimistically stated to illustrate the potential of homogeneous catalysts for controlling selectivity in the aerobic oxidation of lignin.[12] Of interest, an *in situ* Ni(COD)$_2$/*N*-heterocyclic carbene species has been reported to catalyse selective hydrogenolysis of aryl ethers (C–O bond cleavage to phenolic and arene products) in xylene at 120 °C under 1 atm H_2, conditions similar to those used in our Ru systems, although excess NaO^{t}Bu was needed in the carbene system;[28] however, use of a substrate like **9** (but containing two extra OMe substituents), in the basic conditions without the catalyst, gave high conversion to guaiacol and 'numerous products'.

Conclusions

We have confirmed an earlier report[14] that the *in situ* Ru(H)$_2$(CO)(PPh$_3$)$_3$/xantphos system effects the catalytic hydrogenolysis of β-O-4 alcohols such as **1–3**. The known complex Ru(H)$_2$(CO)(PPh$_3$)(xantphos) (**18**)[16] is shown to be the actual precursor catalyst for which an improved synthetic method is presented. The Ru catalyst also effects hydrogenolysis of ketones **4–6** that are shown to be intermediates formed by dehydrogenation of the alcohol substrates. The presence of a γ-OH functionality in the β-O-4 substrates (**7–9**) inhibits their hydrogenolysis because the substrate interacts with 'Ru(CO)(xantphos)' to form catalytically inactive acyl complexes **20** and **21** that contain tridentate xantphos (with *trans* P-atoms), with a Ru–(CO)–CH═

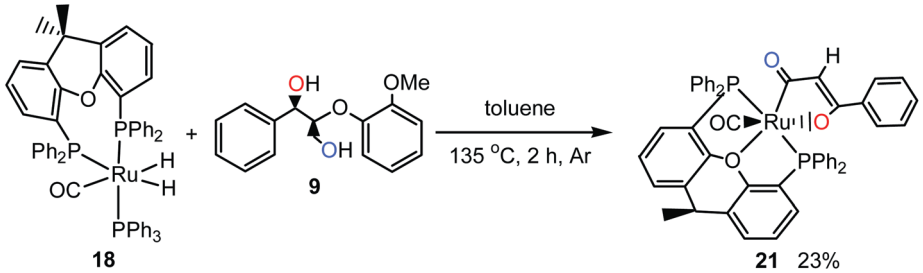

Scheme 8 Reaction of **18** with **9** to form **21**.

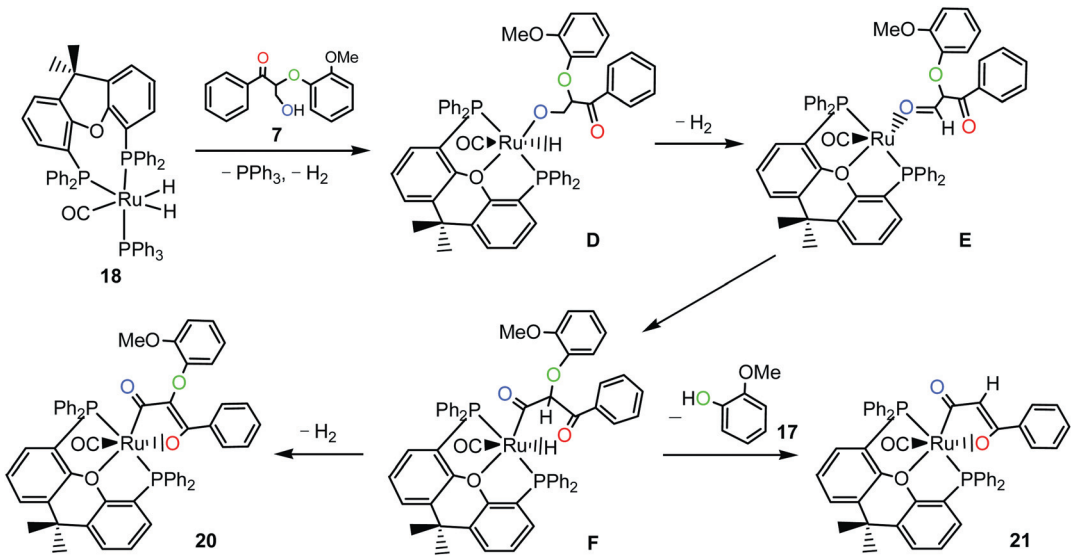

Scheme 9 Proposed mechanism for formation of **20** and **21** from reaction of **7** with **18**.

moiety that involves the original γ-carbon atom of the substrates. This may be relevant in the lack of activity of **18** toward lignin samples which possess β-O-4/γ-OH linkages. Current work involves modification of the γ-OH functionality in models such as **7–9**, with the hope of more success in catalysed breakdown reactions of lignin.

Experimental

General

NMR spectra were recorded at r.t., unless noted otherwise, on Bruker spectrometers (300, 400, or 600 MHz for ^{1}H; 75, 100, or 150 MHz for $^{13}C\{^{1}H\}$; and 122 MHz for $^{31}P\{^{1}H\}$). Residual deuterated solvent protons (relative to external $SiMe_4$)[41] or external 85% H_3PO_4 was used as reference (s = singlet, d = doublet, t = triplet, q = quartet, m = multiplet, ps = pseudo; *J* values are given in Hz). Deuterated solvents were purchased from Cambridge Isotope Laboratories, Inc. IR, $\nu_{C\equiv O}$ bands were recorded (in cm^{-1}) on a Perkin Elmer Frontier FT-IR spectrometer using an ATR sampling surface. Electrospray ionization mass spectra in the positive ion mode (ESI/MS^{+}) were recorded on a Bruker Esquire-LC ion trap instrument, with MeOH solution of samples being infused into the ion-source by a syringe pump at a flow rate of 200 μL min^{-1}. Elemental analyses were performed using a Carlo Erba EA1108 elemental analyzer.

All general solvents and reagents used in the syntheses were 'reagent grade' and were used as supplied by Aldrich or Fisher Scientific. Silica gel (SiliaFlash® F60, 230–400 mesh) was purchased from Silicycle, and the Praxair gases H_2 (99.995%, extra dry), Ar (99.996%), and N_2 (99.998%) were used as received.

Literature reported compounds

The following compounds were synthesized by literature methods: $Ru(H)_2(CO)(PPh_3)_3$,[42] 2-(2-methoxyphenoxy)-1-phenylethanol (**1**),[14] 2-(2-methoxyphenoxy)-1-phenylethanone (**4**),[14] 1-(4-ethoxy-3-methoxyphenyl)-2-(2-methoxyphenoxy)-ethanone (**5**),[11] and 1-(4-ethoxy-3-methoxyphenyl)-3-hydroxy-2-(2-methoxyphenoxy)-1-propanone (**8**).[11] The syntheses of **3**, and **10–12**, described below, are modifications of the noted literature methods. The modifications include use of: a one- *versus* two-step procedure, different solvents, temperatures, reaction times, and purification methods.

1-(4-Ethoxy-3-methoxyphenyl)-2-(2-methoxyphenoxy)ethanol (2). To a stirred THF/H_2O (50 mL/12 mL) solution of **5** (2.5 g, 7.9 mmol), $NaBH_4$ (0.66 g, 17 mmol) was added over 5 min, and the stirring was continued for 3 h at r.t. Saturated aq. NH_4Cl

(50 mL), H_2O (50 mL) and THF (50 mL) were then added; the organic layer was subsequently collected, and the aq. layer was extracted with Et_2O (2 × 50 mL). The organic layers were combined, washed with brine (2 × 50 mL), dried over $MgSO_4$, and filtered. The filtrate was evaporated to give a white powder that was dried *in vacuo*. Yield = 1.9 g (77%). ^{1}H NMR (600 MHz, $CDCl_3$): δ 1.46 (OCH_2CH_3, t, 3H, J = 7.2), 3.75 (OH, s, 1H), 3.87 and 3.88 (OCH_3, s, 3H each), 3.97 (C*H*H, t, 1H, J = 10), 4.09 (OCH_2CH_3, q, 2H, J = 6.6), 4.15 (CH*H*, dd, 1H, J = 9.6, 3.0), 5.05 (C*H*OH, dd, 1H, J = 9.9, 3.0), 6.83–7.03 (Ar–H, m, 7H). ^{13}C{^{1}H} NMR (150 MHz, $CDCl_3$): δ 14.90 (OCH_2CH_3), 55.91 (OCH_3), 56.01 (OCH_3), 64.44 (OCH_2CH_3), 72.18 (*C*HOH), 76.23 (CH_2), 109.71, 112.00, 112.56, 115.67, 118.69, 121.19, 122.45, 132.21, 148.06, 148.11, 149.43, 150.00. ESI/MS$^+$: 341 [M + Na]$^+$. Anal. Calcd for $C_{18}H_{22}O_5 \cdot H_2O$: C, 64.27; H, 7.19. Found: C, 64.3; H, 7.2.

4-Benzoyl-3-methoxy-bromoacetylbenzene (10).[25,27] Benzoyl chloride (19 g, 0.14 mol) and pyridine (11 g, 0.14 mol) were added drop-wise to a stirred reaction mixture of acetovanillone (20 g, 0.12 mol) in $CHCl_3$ (100 mL) at r.t. After 1 h, the solvent was removed and the residue was extracted with EtOAc (2 × 100 mL). This solvent was then removed, and the residue was dissolved in $CHCl_3$ (100 mL). Br_2 (19 g, 0.12 mol) was then added drop-wise, and the mixture was then stirred for 16 h at r.t. Subsequent evaporation of the solvent gave a white solid that was recrystallized from hexanes–EtOAc (7 : 3, 200 mL), filtered off, washed with hexanes (2 × 40 mL), and dried *in vacuo*. Yield = 30 g (74%). ^{1}H NMR (400 MHz, $CDCl_3$): δ 3.89 (OCH_3, s, 3H), 4.46 (CH_2, s, 2H), 7.28 (Ar–H, d, 1H, J = 8.4), 7.53 (Ar–H, t, 2H, J = 7.6), 7.61–7.69 (Ar–H, m, 3H), 8.21 (Ar–H, d, 2H, J = 6.8); the data agree with those reported.[25,27] ^{13}C{^{1}H} NMR (100 MHz, $CDCl_3$): δ 30.69 (CH_2Br), 56.29 (OCH_3), 112.52, 122.54, 123.35, 128.77, 128.95, 130.52, 132.84, 133.98, 144.95, 152.09, 164.28 (O═C–O), 190.42 (O═*C*CH_2). ESI/MS$^+$: 371 [M + Na]$^+$. Anal. Calcd for $C_{16}H_{13}O_4Br$: C, 55.04; H, 3.75. Found: C, 55.0; H, 3.7.

1-(4-Benzoyl-3-methoxyphenyl)-2-(2-methoxyphenoxy)-ethanone (11).[25,27] Guaiacol (2.2 g, 18 mmol) was added drop-wise to a stirred acetone solution (150 mL) of K_2CO_3 (2.5 g, 18 mmol) and **10** (5.0 g, 14 mmol) at r.t. After 16 h, the solid was filtered off, and the filtrate was evaporated to give a residue that was loaded onto a silica gel column; hexanes–EtOAc (7 : 3) was used as elutant. The appropriate fractions were collected and evaporated to yield a white powder that was washed with hexanes–EtOAc (7 : 3, 2 × 20 mL) and then dried *in vacuo*. Yield = 1.8 g (32%). ^{1}H NMR (400 MHz, $CDCl_3$): δ 3.88 and 3.89 (OCH_3, s, 3H each), 5.34 (CH_2, s, 2H), 6.83–7.03 (Ar–H, m, 4H), 7.27 (Ar–H, d, 1H, J = 8.4), 7.52 (Ar–H, t, 2H, J = 8.0), 7.62–7.75 (Ar–H, m, 3H), 8.21 (Ar–H, d, 2H, J = 6.8); the data agree with those reported.[23,25] ^{13}C{^{1}H} NMR (100 MHz, $CDCl_3$): δ 56.01 (OCH_3), 56.26 (OCH_3), 72.35 (CH_2), 112.05, 112.32, 115.05, 120.96, 121.53, 122.71, 123.39, 128.75, 129.01, 130.52, 133.52, 133.93, 144.73, 147.53, 149.92, 152,01, 164.33 (O═C–O), 193.76 (O═*C*CH_2). ESI/MS$^+$: 415 [M + Na]$^+$. Anal. Calcd for $C_{23}H_{20}O_6$: C, 70.40; H, 5.14. Found: C, 69.9; H, 5.1

1-(4-Hydroxy-3-methoxyphenyl)-2-(2-methoxyphenoxy)ethanol (3).[27] $NaBH_4$ (0.32 g, 8.5 mmol) was added over 5 min to a stirred mixture of NaOH (3.0 g, 75 mmol) and **11** (1.5 g, 3.8 mmol) in THF/H_2O (50 mL/50 mL) at r.t. After 16 h, aq. NH_4Cl (100 mL) and THF (50 mL) were added; the organic layer was collected, and the aq. layer was extracted with Et_2O (2 × 50 mL). The organic layers were combined, dried over $MgSO_4$, and then filtered. The filtrate was evaporated to give a residue that was dissolved in minimum CH_2Cl_2 and loaded onto a silica gel column; hexanes–EtOAc (7 : 3) was used as elutant. The appropriate fractions were collected and evaporated to yield a white solid that was washed with hexanes–EtOAc (7 : 3, 2 × 20 mL), collected, and dried *in vacuo*. Yield = 0.43 g (39%). ^{1}H NMR (600 MHz, $CDCl_3$): δ 3.45 (CHO*H*, s, 1H), 3.89 and 3.90 (OCH_3, s, 3H each), 3.96 (C*H*H, t, 1H, J = 10), 4.16 (CH*H*, dd, 1H, J = 9.9, 3.0), 5.03 (C*H*OH, d, 1H, J = 9.0), 5.64 (Ar–OH, s, 1H), 6.85–7.06 (Ar–H, m, 7H); the data agree with those reported.[25] ^{13}C{^{1}H} NMR (150 MHz, $CDCl_3$): δ 55.98 (OCH_3), 56.06 (OCH_3), 72.29 (CHOH), 76.56 (CH_2), 108.86, 112.07, 114.34, 116.20, 119.48, 121.22, 122.71, 131.61, 145.53, 146.76, 148.10, 150.29. ESI/MS$^+$: 313 [M + Na]$^+$. Anal. Calcd for $C_{16}H_{18}O_5 \cdot 0.3H_2O$: C, 64.99; H, 6.34. Found: C, 65.0; H 6.1.

1-(4-Hydroxy-3-methoxyphenyl)-2-(2-methoxyphenoxy)-ethanone (6). The procedure was identical to that used for the synthesis of **3**, the corresponding alcohol, but with omission of the $NaBH_4$ treatment. The fraction containing **6** from the silica gel column was initially obtained as a colourless oil, but drying *in vacuo* gave a white solid. Yield = 0.37 g (34%). ^{1}H NMR (600 MHz, $CDCl_3$): δ 3.88 and 3.93 (OCH_3, s, 3H each), 5.29 (CH_2, s, 2H), 6.22 (OH, s, 1H), 6.81–6.87 (Ar–H, m, 2H), 6.88–6.99 (Ar–H, m, 3H), 7.58–7.64 (Ar–H, m, 2H). ^{13}C{^{1}H} NMR (150 MHz, $CDCl_3$): δ 55.98 (OCH_3), 56.19 (OCH_3), 71.96 (CH_2), 110.24, 112.19, 114.12, 114.67, 120.89, 122.41, 123.43, 127.61, 146.92, 147.64, 149.76, 151.07, 193.24 (C═O). ESI/MS$^+$: 311 [M + Na]$^+$. Anal. Calcd for $C_{16}H_{16}O_5 \cdot 0.5H_2O$: C, 64.64; H, 5.76. Found: C, 64.5; H, 5.4.

3-Hydroxy-2-(2-methoxyphenoxy)-1-phenyl-1-propanone (7). A 1 : 1 EtOH–acetone solution (30 mL) containing **4** (1.00 g, 4.13 mmol), K_2CO_3 (685 mg, 4.96 mmol), and formaldehyde (516 mg, 6.36 mmol, purchased as a 37% by weight aq. solution with ~10% MeOH) was stirred for 2 h at r.t. The solvent was evaporated off to leave a residue that was extracted with CH_2Cl_2. The extracts were purified *via* silica gel chromatography (2 : 1 hexanes–EtOAc), the appropriate fractions being collected, evaporated to dryness, and re-precipitated with CH_2Cl_2/hexanes to yield a white solid that was collected and dried *in vacuo*. Yield = 290 mg (26%). ^{1}H NMR (400 MHz, $CDCl_3$): δ 3.03 (OH, t, 1H, J = 6.2), 3.85 (OCH_3, s, 3H), 4.07 ($HOCH_2$, m, 2H), 5.44 (CH, t, 1H, J = 5.2), 6.83 (Ar–H, t, 1H, J = 7.8), 6.92 (Ar–H, d, 2H, J = 7.2), 7.02 (Ar–H, t, 1H, J = 7.6), 7.48 (Ar–H, t, 2H, J = 7.6), 7.60 (Ar–H, t, 1H, J = 7.4), 8.06 (Ar–H, d, 2H, J = 7.2). ^{13}C{^{1}H} NMR (100 MHz, $CDCl_3$): δ 55.95 (OCH_3), 63.57 ($HOCH_2$), 85.00 (CH), 112.51, 119.05, 121.35, 123.95, 128.93, 133.92, 135.14, 147.05, 150.71, 196.75 (C═O). ESI/MS$^+$: 295 [M + Na]$^+$. Anal Calcd for $C_{16}H_{16}O_4 \cdot 0.5H_2O$: C, 68.31; H, 6.09. Found: C, 68.3; H, 6.1.

Methyl 2-(2-methoxyphenoxy)acetate (12).[28] Methyl bromoacetate (10 g, 65 mmol) and guaiacol (7.4 g, 60 mmol) were added drop-wise to a stirred mixture of K_2CO_3 (9.0 g, 65 mmol)

in 60 mL acetone. After being refluxed at 70 °C for 2 h, the mixture was cooled to r.t. and was filtered. Evaporation of the solvent from the filtrate left a colourless oil; hexanes (5 mL) were added and on being cooled at −15 °C for ∼12 h the solution deposited colorless crystals that were collected, washed with hexanes (2 × 10 mL), and dried *in vacuo*. Yield = 4.0 g (34%). ^{1}H NMR (300 MHz, $CDCl_3$): δ 3.78 and 3.87 (OCH_3, s, 3H each), 4.69 (CH_2, s, 2H), 6.76–7.04 (Ar–H, m, 4H). $^{13}C\{^1H\}$ NMR (75 MHz, $CDCl_3$): δ 52.16 (OCH_3), 55.85 (OCH_3), 66.46 (CH_2), 112.12, 114.43, 120.74, 122.59, 147.21, 149.66, 169.50 (C═O). The NMR data agree with those reported.[28] ESI/MS$^+$: 219 $[M + Na]^+$. Anal. Calcd for $C_{10}H_{12}O_4$: C, 61.22; H, 6.16. Found: C, 61.3; H, 6.2.

Methyl 3-hydroxy-2-(2-methoxyphenoxy)-3-phenylpropanoate (13). Compound **12** (4.0 g, 20 mmol) was placed in a Schlenk flask fitted with a septum. The flask was evacuated, and then filled with flowing Ar. THF (60 mL) was added, and the mixture was stirred, and cooled to −78 °C. LDA·THF (15 mL, 23 mmol, of a 1.5 M cyclohexane solution) was added and, after 10 min, benzaldehyde (2.1 g, 20 mmol) in THF (20 mL) was added; the mixture was then stirred for 2 h at −78 °C under Ar, when saturated aq. NH_4Cl (75 mL) was added (in air). The organic layer of the contents was subsequently collected at r.t., and the aq. layer was extracted with EtOAc (3 × 50 mL). The organic layers were combined, dried over $MgSO_4$, and filtered; evaporation of the filtrate yielded a yellow oil that was purified *via* silica gel chromatography (2 : 1 hexanes–EtOAc). The appropriate fraction was collected, and rotary evaporation of the appropriate fraction gave a yellow oil that on treatment with CH_2Cl_2/hexanes (5 mL/50 mL) at −15 °C precipitated after 16 h a white powder that was collected, washed with hexanes (2 × 10 mL), and dried *in vacuo*. Yield = 1.3 g (21%). ^{1}H NMR (400 MHz, $CDCl_3$): δ 3.66 and 3.86 (OCH_3, s, 3H each), 3.83 (OH, d, 1H, J = 6.4), 4.77 (CHC═O, d, 1H, J = 4.8), 5.20 (C*H*OH, ps t, 1H, J = 5.4), 6.84 (Ar–H, t, 1H, J = 7.8), 6.88–6.95 (Ar–H, m, 2H), 7.03 (Ar–H, t, 1H, J = 7.6), 7.28–7.48 (Ar–H, m, 5H). $^{13}C\{^1H\}$ NMR (100 MHz, $CDCl_3$): δ 52.19 (OCH_3), 56.02 (OCH_3), 74.19 (COH), 84.34 (*C*C═O), 112.47, 119.48, 121.29, 124.31, 126.87, 128.24, 128.35, 139.11, 147.23, 150.83, 169.84 (C═O). ESI/MS$^+$: 325 $[M + Na]^+$. Anal. Calcd for $C_{17}H_{18}O_5$: C, 67.54; H, 6.00. Found: C, 67.2; H, 6.0.

2-(2-Methoxyphenoxy)-1-phenyl-1,3-propanediol (9). $NaBH_4$ (0.58 g, 15 mmol) was added over 5 min to a THF/H_2O (30 mL/10 mL) solution of **13** (0.92 g, 3.0 mmol) that was left stirring for 22 h at r.t. After addition of a saturated aq. NH_4Cl (50 mL), EtOAc (50 mL) was then added. The organic layer was collected, and the aq. layer was extracted with Et_2O (2 × 50 mL). The combined organic layers were dried over $MgSO_4$; evaporation of the filtrate gave a yellow oil that was dried *in vacuo* at 50 °C. Yield = 0.65 g (76%). ^{1}H NMR (600 MHz, $CDCl_3$) for the major diastereomer: δ 2.96 (CH_2OH, t, 1H, J = 6.0), 3.61–3.69 (C*H*HOH, m, 1H), 3.76 (CHO*H*, d, 1H, J = 3.0), 3.88 (OCH_3, s, 3H), 3.91–3.96 (CH*H*OH, m, 1H), 4.18–4.22 (C*H*CH_2, m, 1H), 5.06 (C*H*OH, ps t, 1H, J = 3.6), 6.88–6.99 (Ar–H, m, 3H), 7.07 (Ar–H, t, 1H, J = 7.8), 7.29 (Ar–H, t, 1H, J = 7.8), 7.36 (Ar–H, t, 2H, J = 7.5), 7.39 (Ar–H, d, 2H, J = 7.8). $^{13}C\{^1H\}$ NMR (150 MHz, $CDCl_3$): δ 55.98 (OCH_3), 60.67 (CH_2OH), 72.99 (CHOH), 87.34 (*C*HCH_2), 112.27, 121.02, 121.71, 124.29, 126.18, 127.75, 128.49, 140.00, 146.88, 151.66. ESI/MS$^+$: 297 $[M + Na]^+$. Anal. Calcd for $C_{16}H_{18}O_4$: C, 70.06; H, 6.61. Found: C, 69.5; H, 6.7. The NMR data agree with those reported in acetone-d_6 for **9**, synthesized by a different route.[30]

Ru(H)$_2$(CO)(PPh$_3$)(xantphos) (18).[16] Complex **18** was prepared essentially *via* the literature method,[16] but with one major modification in that an H_2 atmosphere was used rather than the reported Ar; in our hands, use of Ar did not yield **18**.

$Ru(H)_2(CO)(PPh_3)_3$ (0.25 g, 0.27 mmol), xantphos (0.19 g, 0.33 mmol), and toluene (5 mL) were charged in a Schlenk flask, which after three freeze–pump–thaw cycles was filled with H_2 to 1 atm. The mixture was heated with stirring at 120 °C for 2 h, and then cooled to r.t. Addition of hexanes (50 mL) precipitated a yellow powder that was collected, washed with hexanes (2 × 10 mL), and dried *under vacuo* at 70 °C. Yield = 0.15 g (58%). ^{1}H NMR (300 MHz, toluene-d_8): δ −8.73 (Ru–H, m, 1H), −6.68 (Ru–H, m, 1H), 1.38 and 1.51 (CH_3, s, 3H each), 6.40–7.90 (Ar–H, m, 26H). $^{31}P\{^1H\}$ NMR (122 MHz, toluene-d_8): δ 30.6–31.3 (xantphos-P, m), 44.0–47.6 (xantphos-P, m), 59.4 (PPh_3, dd, J = 241, 16). IR: 1948 ($\nu_{C\equiv O}$). ESI/MS$^+$: 971 $[M - H]^+$. Anal. Calcd for $C_{58}H_{49}O_2P_3Ru$: C, 71.67; H, 5.08. Found: C, 71.4; H, 5.1. All the analytical data agree with those reported.[16]

Catalysed reactions of lignin substrates

The lignin model substrate **1–9** (0.10 mmol), the catalyst (5 mol% of one of the following: **18**, $Ru(H)_2(CO)(PPh_3)_3$ + xantphos, $Ru(H)_2(CO)(PPh_3)_3$), and toluene-d_8 (0.5 mL), were added to a J-Young NMR tube. After three freeze–pump–thaw cycles, the tube was filled with 1 atm of H_2 or Ar; for N_2, a glove-box procedure was used. ^{1}H NMR spectra were recorded at r.t., prior to and after the reaction (20 h at 135 °C), with pivalic acid (5–15 mg, 0.05–0.15 mmol) being used as an external standard for determination of product yields and substrate conversions. The relevant δ_H values used for toluene-d_8 solutions are: for **1** (3.32, OCH_3, s), **2** (3.34, 2-OCH_3, s), **3** (3.34, 2-OCH_3, s), **4** (4.79, CH_2, s), **5** (4.91, CH_2, s), **6** (4.85, CH_2, s), **7** (5.34, CH, t), **8** (5.42, CH, t), **9** (4.12, C*H*CH_2, m), **14** (2.07, CH_3, s), **15** (2.22, CH_3, s), **16** (2.15, CH_3, s), **17** (3.19, OCH_3, s), 1-phenylethanol (1.31, CH_3, d), pivalic acid (1.07, $(CH_3)_3$, s).

Ru(CO)(xantphos)(OC$_6$H$_4$O) (19). Catechol (100 mg, 0.91 mmol), **18** (90 mg, 0.093 mmol), and toluene (5 mL) were mixed in a Schlenk flask, which after three freeze–pump–thaw cycles was filled with Ar to 1 atm. Reaction at 135 °C for 18 h yielded a yellow precipitate that was collected, washed with hexanes (2 × 10 mL), and dried *in vacuo*. Yield = 50 mg (66%) of a ∼1 : 1 mixture of isomers (see text). ^{1}H NMR (300 MHz, CD_2Cl_2): δ 1.56, 1.71, 1.78, 1.92 (CH_3, s), 6.10–7.80 (Ar–H, m). $^{31}P\{^1H\}$ NMR (122 MHz, CD_2Cl_2): δ 49.9, 55.1. IR: 1921 ($\nu_{C\equiv O}$). ESI/MS$^+$: 816 $[M + H]^+$. Anal. Calcd for $C_{46}H_{36}O_4P_2Ru$: C, 67.72; H, 4.45. Found: C, 68.1; H, 4.6.

Ru(CO)(xantphos)[C(O)C(OC$_6$H$_4$OMe)═C(Ph)O] (20). The synthesis was similar to that given for **19**, but using substrate **7** (140 mg, 0.51 mmol) with **18** (100 mg, 0.10 mmol) and a reaction time of 2 h; the white precipitate was collected and dried

in vacuo at 70 °C. Yield = 34 mg (34%). ^{1}H NMR (300 MHz, CD_2Cl_2): δ 1.78 and 1.98 (xantphos-CH_3, s, 3H each), 3.80 (OCH_3, s, 3H), 5.50 (Ar–H, d, 1H, J = 8.1), 6.16 (Ar–H, t, 1H, J = 7.5), 6.64 (Ar–H, t, 1H, J = 7.1), 6.75 (Ar–H, d, 1H, J = 7.8), 6.94–7.54 (Ar–H, m, 25H), 7.64–7.84 (Ar–H, m, 6H). ^{31}P{^{1}H} NMR (122 MHz, CD_2Cl_2): δ 32.1. IR: 1947 ($\nu_{C\equiv O}$). ESI/MS$^+$: 977 $[M + H]^+$, 999 $[M + Na]^+$. Anal. Calcd for $C_{56}H_{44}O_6P_2Ru{\cdot}H_2O$: C, 67.67; H, 4.66. Found: C, 67.8; H, 4.5.

Ru(CO)(xantphos)[C(O)CH=C(Ph)O] (21). This complex was isolated from the filtrate obtained from the synthesis of **20**, with the filtrate being transferred to a flask. Removal of the solvent yielded an oil that was purified *via* silica gel chromatography (1 : 1 hexanes–EtOAc to neat EtOAc), the appropriate fractions being collected, evaporated to dryness, and re-precipitated with C_6H_6/hexanes (5 mL/50 mL) to yield a white powder that was collected, washed with hexanes (2 × 10 mL), and dried *in vacuo*. Yield = 27 mg (31%). ^{1}H NMR (300 MHz, CD_2Cl_2): δ 1.73 and 1.97 (xantphos-CH_3, s, 3H each), 4.95 (CH=C, s, 1H), 6.80–7.90 (Ar–H, m, 31H). ^{31}P{^{1}H} NMR (122 MHz, CD_2Cl_2): δ 35.0. IR: 1947 ($\nu_{C\equiv O}$). ESI/MS$^+$: 855 $[M + H]^+$. Anal. Calcd for $C_{49}H_{38}O_4P_2Ru{\cdot}H_2O$: C, 67.50; H, 4.62. Found: C, 67.3; H, 4.6.

X-ray structural determinations

X-ray analyses were carried out at −173 or −183 °C on a Bruker APEX DUO diffractometer with Cu-Kα radiation of 1.54178 Å (for **13**) or a Bruker X8 APEX II diffractometer with graphite monochromated Mo-Kα radiation of 0.71073 Å (for **19–21**). For **13** and **20**, the data for were processed using the Bruker SAINT software package,[43] and corrected for absorption effects using the multi-scan technique (SADABS),[44] as well as for Lorentz and polarization effects. All the structures were solved by direct methods,[45] with all non H-atoms being refined anisotropically; the H-atoms were placed in calculated positions. Refinements for **13** and **20** were performed using the SHELXL-97[46] *via* the WinGX interface.[47]

Complex **19** crystallized as a twin crystal with the two components related by a 180° rotation about the (1 0 −1) real axis. Data were integrated using the SAINT software[43] for both components, including both overlapped and non-overlapped reflections, with the correction for absorption effects done with the multi-scan technique (TWINABS).[47] The direct methods[45] now used the non-overlapped data from the major twin component, and subsequent refinements were carried out using an HKLF 4 format data set containing complete data from the other component. The material crystallizes with one half molecule in the asymmetric unit, with the two halves related by mirror symmetry; in addition, half a molecule of the CH_2Cl_2 molecule is seen in the asymmetric unit.

Complex **21** crystallized as a "split-crystal" with three components, one and two being related by a 173.8° rotation about the (0.00 1 0.00) reciprocal axis, and three and one being related by a 179.9° rotation about the (−0.01 0 1) reciprocal axis. The SAINT software[43] was then used for integration of all the twin components, with absorption corrections done using TWINABS[47] as described above for **19**. The direct methods[45] now used the non-overlapped data from the major twin component. Two crystallographically independent molecules exist in the asymmetric unit. Subsequent refinements were carried out using an HKLF 5 format data set containing complete data from component one and any overlapped reflections from components two and three. Constraints were applied to all phenyl rings to ensure that they maintained reasonable geometries.

Acknowledgements

We thank NSERC Lignoworks for funding, Prof. Laurel Schafer – a colleague here at UBC – for providing some laboratory equipment (particularly use of a glove-box), and her postdoctoral fellows Christine Rogers, Zhengxing Zhang, and Patricia Horrillo-Martinez for discussions.

Notes and references

1 (*a*) J. Zakzeski, P. C. A. Bruijnincx, A. L. Jongerius and B. M. Weckhuysen, *Chem. Rev.*, 2010, **110**, 3552 and refs. therein; (*b*) S. R. Collinson and W. Thielemans, *Coord. Chem. Rev.*, 2010, **254**, 1854 and refs. therein.
2 S. K. Hanson, R. Wu and L. A. Silks, *Angew. Chem., Int. Ed.*, 2012, **51**, 3410 and refs. therein.
3 J. R. Regalbuto, *Science*, 2009, **325**, 822.
4 (*a*) W. G. Glasser, R. A. Northey and T. P. Schultz, *Lignin: Historical, Biological, and Materials Perspectives*, Am. Chem. Soc., Washington, DC, 2000; (*b*) D. Mohan, C. Pittman Jr. and P. H. Steele, *Energy Fuels*, 2006, **20**, 848; (*c*) M. Kleinert and T. Barth, *Chem. Eng. Technol.*, 2008, **31**, 736.
5 (*a*) G. Brunow, in *Biopolymers, Lignin, Humic Substances and Coal*, ed. A. Steinbuchel, M. Hofrichter, Wiley-VCH, Weinheim, Germany, 2001, vol. 1, p. 89; (*b*) L. B. Davin and N. G. Lewis, *Curr. Opin. Biotechnol.*, 2005, **16**, 407.
6 Y. S. Kim, H.-M. Chang and J. F. Kadla, *Holzforschung*, 2008, **62**, 38.
7 These models are not strictly dimers – they are comprised of two non-identical aromatic units.
8 M. E. Brown, M. C. Walker, T. G. Nakashige, A. T. Iavarone and M. C. Y. Chang, *J. Am. Chem. Soc.*, 2011, **133**, 18006.
9 S. K. Badamali, R. Luque, J. H. Clark and S. W. Breeden, *Catal. Commun.*, 2011, **12**, 993.
10 S. Jia, B. J. Cox, X. Guo, Z. C. Zhang and J. G. Ekerdt, *Ind. Eng. Chem. Res.*, 2011, **50**, 849.
11 S. Son and F. D. Toste, *Angew. Chem., Int. Ed.*, 2010, **49**, 3791.
12 B. Sedai, C. Díaz-Urrutia, R. T. Baker, R. Wu, L. A. Silks and S. K. Hanson, *ACS Catal.*, 2011, **1**, 794.
13 S. K. Hanson, R. T. Baker, J. C. Gordon, B. L. Scott and D. L. Thorn, *Inorg. Chem.*, 2010, **49**, 5611.
14 J. M. Nichols, L. M. Bishop, R. G. Bergman and J. A. Ellman, *J. Am. Chem. Soc.*, 2010, **132**, 12554.
15 (*a*) A. E. W. Ledger, M. F. Mahon, M. K. Whittlesey and J. M. J. Williams, *Dalton Trans.*, 2009, 6941; (*b*) L. M. Guard, A. E. W. Ledger, S. P. Reade, C. E. Ellul, M. F. Mahon and M. K. Whittlesey, *J. Organomet. Chem.*, 2011, **696**, 780.
16 A. E. W. Ledger, P. A. Slatford, J. P. Lowe, M. F. Mahon, M. K. Whittlesey and J. M. J. Williams, *Dalton Trans.*, 2009, 716.
17 (*a*) A. E. W. Ledger, A. Moreno, C. E. Ellul, M. F. Mahon, P. S. Pregosin, M. K. Whittlesey and J. M. J. Williams, *Inorg. Chem.*, 2010, **49**, 7244; (*b*) A. E. W. Ledger, C. E. Ellul, M. F. Mahon, J. M. J. Williams and M. K. Whittlesey, *Chem.–Eur. J.*, 2011, **17**, 8704.
18 A. N. Kharat, A. Bakhoda and B. T. Jahromi, *Inorg. Chem. Commun.*, 2011, **14**, 1161.
19 P. Nieczypor, P. W. N. M. van Leeuwen, J. C. Mol, M. Lutz and A. L. Spek, *J. Organomet. Chem.*, 2001, **625**, 58.
20 P. A. Slatford, M. K. Whittlesey and J. M. J. Williams, *Tetrahedron Lett.*, 2006, **47**, 6787.
21 (*a*) S. J. Pridmore, P. A. Slatford and J. M. J. Williams, *Tetrahedron Lett.*, 2007, **48**, 5111; (*b*) S. J. Pridmore, P. A. Slatford, J. E. Taylor, M. K. Whittlesey and J. M. J. Williams, *Tetrahedron*, 2009, **65**, 8981;

(*c*) S. J. Pridmore, P. A. Slatford, A. Daniel, M. K. Whittlesey and J. M. J. Williams, *Tetrahedron Lett.*, 2007, **48**, 5115.
22 N. Anand, N. A. Owston, A. J. Parker, P. A. Slatford and J. M. J. Williams, *Tetrahedron Lett.*, 2007, **48**, 7761.
23 (*a*) A. J. Blacker, M. M. Farah, M. I. Hall, S. P. Marsden, O. Saidi and J. M. Williams, *Org. Lett.*, 2009, **11**, 2039; (*b*) A. J. A. Watson, A. C. Maxwell and J. M. J. Williams, *Org. Biomol. Chem.*, 2012, **10**, 240.
24 K. Takahashi, M. Yamashita, Y. Tanaka and K. Nozaki, *Angew. Chem., Int. Ed.*, 2012, **51**, 4383.
25 C. Crestini and M. D'Auria, *Tetrahedron*, 1997, **53**, 7877.
26 S. Kawai, K. Okita, K. Sugishita, A. Tanaka and H. Ohashi, *J. Wood Sci.*, 1999, **45**, 440.
27 E. Roznіecka, I. Zawisza, M. Jawiczuk, D. Branowska and M. Opallo, *J. Electroanal. Chem.*, 2010, **645**, 123.
28 A. G. Sergeev and J. F. Hartwig, *Science*, 2011, **332**, 439.
29 (*a*) W. Ibrahim and K. Lundquist, *Acta Chem. Scand.*, 1994, **48**, 149; (*b*) D. W. Cho, R. Parthasarathi, A. S. Pimentel, G. D. Maestas, H. J. Park, U. C. Yoon, D. Dunaway-Mariano, S. Gnanakaran, P. Langan and P. S. Mariano, *J. Org. Chem.*, 2010, **75**, 6549 and refs. therein.
30 K. Li and R. F. Helm, *Holzforschung*, 2000, **54**, 597.
31 These signals are similar to those reported[32] for the orthometallated species Ru(*o*-$C_6H_4PPh_2$)(H)(CO)(PPh_3)$_2$ formed from Ru(H)$_2$(CO)(PPh_3)$_3$, which hints at the possibility of a Ru(CO)(xantphos)-containing species similarly undergoing such intramolecular C–H activation.
32 F. Kakiuchi, T. Kochi, E. Mizushima and S. Murai, *J. Am. Chem. Soc.*, 2010, **132**, 17741.
33 L. S. van der Sluys, G. J. Kubas and K. G. Caulton, *Organometallics*, 1991, **10**, 1033 and refs. therein.
34 J. van Buijtenen, J. Meuldijk, J. A. J. M. Vekemans, L. A. Hulshof, H. Kooijman and A. L. Spek, *Organometallics*, 2006, **25**, 873.
35 (*a*) M. C. van Engelen, H. T. Teunissen, J. G. de Vries and C. J. Elsevier, *J. Mol. Catal. A: Chem.*, 2003, **206**, 185; (*b*) M. B. Ezhova, A. Z. Lu, B. R. James and T. Q. Hu, *Chem. Ind.*, 2005, **104**, 135; (*c*) H. Mehdi, V. Fábos, R. Tuba, A. Bodor, L. T. Mika and I. T. Horváth, *Top. Catal.*, 2008, **48**, 49; (*d*) M. Nagy, K. David, G. J. P. Britovsek and A. J. Ragauskas, *Holzforschung*, 2009, **63**, 513; (*e*) M. Schlaf, M. E. Thibault, D. DiMondo, D. Taher, E. Karimi and D. Ashok, *Int. J. Chem. React. Eng.*, 2009, **7**, A34; (*f*) A. S. Gowda, S. Parkin and F. T. Ladipo, *Appl. Organomet. Chem.*, 2012, **26**, 86.
36 For example: (*a*) E. P. Maris, W. C. Ketchie, M. Murayama and R. J. Davis, *J. Catal.*, 2007, **251**, 281; (*b*) R. Preda, V. I. Pârvulescu, A. Petride, A. Banciu, A. Popescu and M. D. Banciu, *J. Mol. Catal. A: Chem.*, 2002, **178**, 79.
37 G. Ferrando-Miguel, P. Wu, J. C. Huffman and K. G. Caulton, *New J. Chem.*, 2005, **29**, 193.
38 Lignins investigated were: an alkali lignin (from Aldrich), pyrolytic lignin and a CH_2Cl_2 soluble fraction lignin (from Prof. J. Kadla, Faculty of Forestry, Univ. of BC), Indulin AT kraft lignin (from MeadWestvaco Corp.); and a lignin from Lignol Energy Corp.
39 M. Kranenburg, Y. E. M. van der Burgt, P. C. J. Kamer, P. W. N. M. van Leeuwen, K. Goubitz and J. Fraanje, *Organometallics*, 1995, **14**, 3081.
40 L. Benhamou, V. César, N. Lugan and G. Lavigne, *Organometallics*, 2007, **26**, 4673.
41 G. R. Fulmer, A. J. M. Miller, N. H. Sherden, H. E. Gottlieb, A. Nudelman, B. M. Stoltz, J. E. Bercaw and K. I. Goldberg, *Organometallics*, 2010, **29**, 2176.
42 N. Ahmad, J. J. Levison, S. D. Robinson and M. F. Uttley, *Inorg. Synth.*, 1974, **15**, 45.
43 *SAINT, Version 7.60A*, Bruker AXS Inc., Madison, Wisconsin, USA., 1997–2009.
44 *SADABS, Version 2008/1: Bruker Nonius area detector scaling and absorption correction*, Bruker AXS Inc., Madison, Wisconsin, USA, 2008.
45 SIR97: A. Altomare, M. C. Burla, M. Camalli, G. L. Cascarano, C. Giacovazzo, A. Guagliardi, A. G. G. Moliterni, G. Polidori and R. Spagna, *J. Appl. Crystallogr.*, 1999, **32**, 115.
46 G. M. Sheldrick, *Acta Crystallogr., Sect. A: Found. Crystallogr.*, 2008, **64**, 112.
47 WinGX, Version 1.80.05: L. J. Farrugia, *J. Appl. Crystallogr.*, 1999, **32**, 837. TWINABS, Version 2008/4: *Bruker AXS scaling for twinned crystals*, Bruker AXS Inc., Madison, Wisconsin, USA, 2008.

